



# El Niño–Southern Oscillation (ENSO) event reduces CO<sub>2</sub> uptake of an Indonesian oil palm plantation

Christian Stiegler<sup>1</sup>, Ana Meijide<sup>2</sup>, Yuanchao Fan<sup>3</sup>, Ashehad Ashween Ali<sup>1</sup>, Tania June<sup>4</sup>, and Alexander Knohl<sup>1</sup>

<sup>1</sup>Bioclimatology, University of Göttingen, Göttingen, Germany

<sup>2</sup>Agronomy Division, Department of Crop Sciences, University of Göttingen, Göttingen, Germany

<sup>3</sup>NORCE Norwegian Research Centre, Bjerknes Centre for Climate Research, Bergen, Norway

<sup>4</sup>Department of Geophysics and Meteorology, Bogor Agricultural University, Bogor, Indonesia

**Correspondence:** Christian Stiegler (christian.stiegler@biologie.uni-goettingen.de)

Received: 1 February 2019 – Discussion started: 12 February 2019

Revised: 12 June 2019 – Accepted: 5 July 2019 – Published: 31 July 2019

**Abstract.** The El Niño–Southern Oscillation (ENSO) in 2015 was one of the strongest observed in almost 20 years and set the stage for a severe drought and the emergence of widespread fires and related smoke emission over large parts of Southeast Asia. In the tropical lowlands of Sumatra, which were heavily affected by the drought and haze, large areas of tropical rainforest have been converted into oil palm (*Elaeis guineensis* Jacq.) plantations during the past decades. In this study, we investigate the impact of drought and smoke haze on the net ecosystem CO<sub>2</sub> exchange, evapotranspiration, yield and surface energy budget in a commercial oil palm plantation in Jambi province (Sumatra, Indonesia) by using micrometeorological measurements, the eddy covariance method, yield data and a multiple linear regression model (MLRM). With the MLRM we identify the contribution of meteorological and environmental parameters to the net ecosystem CO<sub>2</sub> exchange. During the initial part of the drought, when incoming shortwave radiation was elevated, net CO<sub>2</sub> uptake increased by 50 % despite a decrease in upper-layer soil moisture by 35 %, an increase in air temperature by 10 % and a tripling of atmospheric vapour pressure deficit. Emerging smoke haze decreased incoming solar radiation by 35 % compared to non-drought conditions and diffuse radiation almost became the sole shortwave radiation flux for 2 months, resulting in a strong decrease in net CO<sub>2</sub> uptake by 86 %. Haze conditions resulted in a complete pause of oil palm net carbon accumulation for about 1.5 months and contributed to a decline in oil palm yield by 35 %. With respect to a projected pronounced drying trend over the western Pacific during a future El Niño, our model showed that an in-

crease in drought may stimulate net CO<sub>2</sub> uptake, while more severe smoke haze, in combination with drought, can lead to pronounced losses in productivity and net CO<sub>2</sub> uptake, highlighting the importance of fire prevention.

## 1 Introduction

El Niño–Southern Oscillation (ENSO) is a coupled ocean–atmosphere interaction phenomenon in the equatorial Pacific Ocean and one of the most distinct drivers of seasonal to interannual regional and global climate variability (Wolter and Timlin, 2011). Increasing sea surface temperatures in the eastern and central tropical Pacific Ocean are linked to increases in sea-level air pressure in the western Pacific Ocean, resulting in reduced cloudiness and low precipitation over Southeast Asia (Rasmusson and Carpenter, 1981; Wolter, 1986). Generally, ENSO shows episodic and varying timing, frequencies and amplitudes, but the ENSO during 2015 was the strongest observed in almost 20 years (Lim et al., 2017; Santoso et al., 2017). It set the stage for a severe drought over large parts of Southeast Asia, particularly in Indonesia, which favoured the emergence of widespread and mostly human-induced forest, grassland and peat fires (Betts et al., 2016).

The fires released record-breaking amounts of terrestrially stored carbon as CO<sub>2</sub> into the atmosphere, with a mean daily emission rate of 11.3 Tg CO<sub>2</sub> during September to October 2015 (Huijnen et al., 2016). The recent ENSO elevated the Mauna Loa mean monthly CO<sub>2</sub> concentration for 2015

above 400 ppm for the first time in its measurement history and contributed to the highest annual CO<sub>2</sub> growth rate on record (Betts et al., 2016). The emitted aerosol particles from biomass burning covered large parts of Sumatra, Borneo, the Malay Peninsula and Singapore for several months under a persistent pall of smoke haze.

The regions affected by the smoke haze, especially Indonesia and Malaysia, have undergone substantial land-use changes within the past 2 decades due to the world's hunger for cheap vegetable oil, such as palm oil (Koh et al., 2011). Oil palm (*Elaeis guineensis* Jacq.) emerged as an important cash crop due to the extensive application of palm oil in pharmaceutical, cosmetics and food industries, as well as for bio-fuel (Koh and Ghazoul, 2008; Turner et al., 2018). Indonesia and Malaysia are the world's biggest producers of palm oil. For example, in 2016 and 2017, the two countries contributed 56 % (Indonesia) and 30 % (Malaysia) to the global supply of palm oil (USDA, 2018). In 2015, oil palm plantations in the two countries combined covered 17 million ha (Chong et al., 2017).

Oil palm has a long life cycle of about 25 years (Woittiez et al., 2017) and is adapted to tropical climate with an optimal mean temperature of 24–28 °C. It requires frequent and sufficient precipitation of  $\sim 2000 \text{ mm yr}^{-1}$  and a high level of solar radiation (Bakoumé et al., 2013; Corley and Tinker, 2016). Oil palm shows a distinct reaction to changes in atmospheric and soil parameters, including gradual symptoms of water and heat stress such as inhibited growth (Legros et al., 2009; Cao et al., 2011), snapping off of leaves and drying out of fruit bunches (Bakoumé et al., 2013), reduction in yield (Caliman and Southworth, 1998; Noor et al., 2011), reduction or even pause in carbon dioxide assimilation (Méndez et al., 2012; Jazayeri et al., 2015), and, ultimately, plant death (Maillard et al., 1974).

Aerosol particles from biomass burning generally reduce the amount of sunlight reaching the surface and increase the fraction of diffuse radiation through scattering (Kozlov et al., 2014). Diffuse light conditions up to a certain level enhance plant photosynthesis and evapotranspiration through more uniform through-canopy distribution of photosynthetically active radiation (PAR) (Knohl and Baldocchi, 2008; Kanniah et al., 2012; Heuvelink et al., 2014). Light haze smoke intensities may therefore increase CO<sub>2</sub> uptake, maximum rate of photosynthesis ( $A_{\text{max}}$ ) and evapotranspiration, but during dense haze smoke the effect is reversed due to the overall reduction of incoming PAR (Yamasoe et al., 2006; Moreira et al., 2017). In addition, ambient atmospheric CO<sub>2</sub> increase due to local fires and burning may act as a temporary plant CO<sub>2</sub> fertilisation which, to some extent, may offset reduced plant CO<sub>2</sub> uptake during dense smoke haze (Mathews and Ardiyanto, 2016).

Global warming and consequent regional climate changes, including changes in precipitation patterns and increases in the magnitude and frequency of extreme events, such as drought, ENSO and fires (Neelin et al., 2006; IPCC, 2013;

Jiménez-Muñoz et al., 2016), may severely stress oil palm plantations in the near future (Tangang, 2010; Rowland et al., 2015). It is therefore important to assess how much net ecosystem CO<sub>2</sub> exchange (NEE) would change under such conditions. Model predictions suggest more intense ENSO over the course of the 21st century, which may result in a general drying in the western regions of the Pacific Ocean during El Niño (Power et al., 2013; Cai et al., 2014, 2018; Kim et al., 2014; Keupp et al., 2017). The increasing frequency of ENSO-related drought in Southeast Asia has already caused a decline of 10 %–30 % in palm oil production (Paterson et al., 2017). Projected temperature increase and water stress through enhanced ENSO might further decrease oil palm yield (Oettli et al., 2018) or even lead to detrimental conditions for oil palm growth in some areas in Southeast Asia (Paterson et al., 2017). On the other hand, ENSO is associated with an increase in incoming solar radiation in Indonesia, which can increase CO<sub>2</sub> uptake in a tropical environment (Olchev et al., 2015). However, current studies and modelling approaches lack a holistic understanding of ecosystem response; resilience; and the underlying meteorological, ecological, and biological processes during extreme events, such as drought and smoke haze conditions. The ENSO in 2015 was the first strong climate extreme event after the major land-use conversions on Sumatra from forest into oil palm plantations, but only little is known about how the ENSO-related severe drought and persistent smoke haze influenced oil palm monoculture.

In this study, we therefore aim to (a) quantify land–atmosphere CO<sub>2</sub>, water vapour and turbulent heat exchange over an oil palm plantation using the eddy covariance technique during the 2015 ENSO, (b) analyse the contribution to net ecosystem CO<sub>2</sub> exchange (NEE) of meteorological and environmental parameters using a multiple linear regression model (MLRM), (c) investigate the impact of a possible near-future more severe drought and smoke haze scenario on NEE, and (d) evaluate potential changes in evapotranspiration and energy fluxes to the atmosphere. We hypothesise that (a) oil palm monoculture would reduce net ecosystem CO<sub>2</sub> uptake and maximum photosynthetic rate ( $A_{\text{max}}$ ) during drought and haze and (b) sensible heat fluxes would increase at the cost of evaporative cooling.

## 2 Materials and methods

### 2.1 Study site

The study site is located in a commercial oil palm plantation (1°41'35.0" S, 103°23'29.0" E, 76 m a.s.l.) in the tropical lowlands of Jambi province on Sumatra (Indonesia), approx. 25 km west-southwest of Jambi City (Fig. 1). The landscape is flat with small elevation variations of approx.  $\pm 15 \text{ m}$ . Average mean annual air temperature during the period 1991–2011 was 26.7 °C ( $\pm 0.2 \text{ °C}$  standard deviation) and

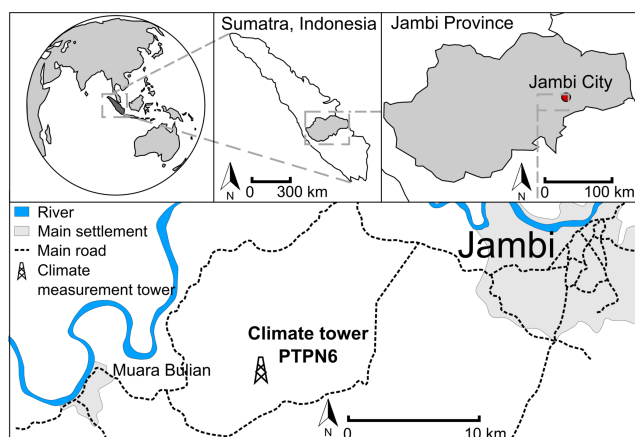


**Figure 1.** Map and location of the study site and climate measurement tower at PTPN6 oil palm plantation, approx. 15 km southwest of the city of Jambi (Sumatra, Indonesia)

mean precipitation for the same period was  $2235 \text{ mm yr}^{-1}$  ( $\pm 381 \text{ mm SD}$ ), with a dry season from June to September and two peak rainy seasons around March and December (Drescher et al., 2016). Long-term climate records are collected at Sultan Thaha Airport, Jambi, approx. 29 km east-northeast of the study site. A comparison of air temperature and precipitation at our study site with climate records from Sultan Thaha Airport, Jambi, during our study period of May 2014 to July 2016 showed no significant differences in daily average air temperature ( $P < 0.001$ ) or in monthly accumulated precipitation ( $P < 0.001$ ). Therefore, we consider the long-term climate records to be representative for our study location.

The oil palm plantation covers 2186 ha and the palm seedlings were planted in the years 1999, 2002 and 2004. Our measurements are located in the section where the palms were planted in 2002. Palms are planted in a triangular array, with  $8 \text{ m} \times 8 \text{ m}$  horizontal density and 156 palms per ha. Based on this horizontal density, an average palm height of 12 m, and 35–45 expanded leaves per palm, Fan et al. (2015) estimated a site-specific leaf area index (LAI) of  $3.64 \text{ m}^2 \text{ m}^{-2}$ . Gaps in oil palms that can be created due to disturbances or extreme weather conditions were not observed in this study. In 2015,  $144 \text{ kg ha}^{-1}$  of magnesium nitrate,  $575 \text{ kg ha}^{-1}$  of nitrogen–phosphorus–potassium (NPK) granular, and  $251 \text{ kg ha}^{-1}$  of dolomite fertilisers were applied in top-dress application. The plantation is owned by Perseroan Terbatas Perkebunan Nusantara VI, Batang Hari Unit (PTPN6). Stumps of pruned oil palm leaves are densely covered with epiphytes, e.g. ferns (Polypodiophyta) or flowering plants (Melastomataceae, Orchidaceae), while understory vegetation is scarce due to regular application of herbicides and occasional mowing. Highly weathered Loam Acrisols soils dominate in the area (Allen et al., 2015) and mean soil carbon and nitrogen content in the plantation reach

$1.12 \%$  ( $\pm 0.34 \%$  SD) and  $0.08 \%$  ( $\pm 0.02 \%$  SD) (Meijide et al., 2017).

## 2.2 Eddy covariance measurements

Eddy covariance (EC) measurements were carried out from June 2014 to July 2016 to derive fluxes of sensible (H) and latent (LE) heat, net ecosystem CO<sub>2</sub> exchange (NEE), and water vapour (ET) for this study. We use a LI7500A fast response open-path CO<sub>2</sub>/H<sub>2</sub>O infrared gas analyser (LI-COR Inc. Lincoln, USA) and a Metek uSonic-3 Scientific sonic anemometer (Metek, Elmshorn, Germany). The EC system measures at 10 Hz and is placed at the top of a 22 m high steel framework tower. Digital signal recording, statistical tests for raw data screening and raw data correction, spectral analysis, eddy flux calculation using EddyPro (LI-COR Inc, Lincoln, USA), post-processing such as quality flagging, removal of fluxes during stable atmospheric conditions, i.e. friction velocity ( $u^* < 0.1 \text{ m s}^{-1}$ ), flux footprint analysis and gap filling of missing flux data follow standard procedures (Meijide et al., 2017). The energy balance closure for the entire study period was 0.75 ( $R^2 = 0.85$ ).

## 2.3 Meteorological and environmental parameters, oil palm yield

Above-ground measurements include air pressure (22 m above the surface), precipitation (11.5 m), wind direction (15.4 m) and wind speed (18.5, 15.4, 13 and 2.3 m), air temperature and air humidity (22, 16.3, 12.3, 8.1, 2.3 and 0.9 m), incoming and reflected photosynthetically active radiation (PAR) (22 m), incoming and outgoing shortwave and longwave radiation (22 m), global and diffuse radiation (22 m), and sunshine duration (22 m). Detailed information on instrument type and manufacturer for all measured parameters can be found in Meijide et al. (2017). Below-ground measurements consist of three profiles where ground heat flux ( $G$ ) is measured with heat flux plates at 5 cm depth and soil moisture and soil temperature is measured at 0.3, 0.6 and 1 m depth, respectively. All meteorological and environmental parameters were measured every 15 s and stored as 10 min mean, minimum and maximum values in a DL16 Pro data logger (Thies Clima, Göttingen, Germany). Monthly oil palm yield data were provided by PTPN6 and cover the period January 2013 to April 2017.

## 2.4 Data analysis and statistics

The meteorological data used in this study cover the period from May 2014 to July 2016. Based on precipitation and the ratio between diffuse and global radiation ( $R_G$ ), i.e. fraction of diffuse radiation (fdifRad), we defined four distinct meteorological periods during 2015, i.e. pre-drought, non-haze drought, haze drought, and post-haze, and compared the four periods with meteorological conditions in 2014 and 2016. We consider pre-drought as the period with frequent

precipitation on an almost daily basis and non-haze drought as the period when precipitation occurred only sporadically and heavy precipitation events of  $> 50 \text{ mm d}^{-1}$  were completely absent. The haze drought period follows the non-haze drought. We defined the start of the haze drought period at the day when daily average fraction of diffuse radiation was  $> 0.8$  for more than 3 consecutive days. We consider the end of the haze drought period as the day when daily average fraction of diffuse radiation dropped below 0.8 for 5 consecutive days and when clear day-to-day variations in fraction of diffuse radiation, with day-to-day variation of  $> 0.2$  became apparent. Reference meteorological conditions cover the period May–December 2014 and January–July 2016.

To investigate the behaviour of the oil palm plantation in more detail, we defined day (06:00–18:30 LT), night (19:00–05:30 LT) and midday (10:00–14:00 LT) time periods. Due to the proximity of our study site to the Equator the difference in day length between summer and winter solstice is only 12 min. Therefore, we consider the impact of differences in day length on the fluxes and meteorological parameters as negligible.

Maximum rate of photosynthesis ( $A_{\text{max}}$ ) at the ecosystem scale was calculated from daily light response curve using NEE (Falge et al., 2001). Initially, we applied CO<sub>2</sub> flux partitioning of NEE into gross primary production (GPP) and respiration using (a) non-linear regression model based on Reichstein et al. (2005) and (b) CO<sub>2</sub> flux partitioning based on CLM-Palm (Fan et al., 2015), which is a sub-model within the framework of the Community Land Model (CLM4.5) (Oleson et al., 2013). The non-linear regression model underestimated NEE by 58 %, on average, most likely because the model struggles to assess the temperature sensitivity of ecosystem respiration using the filtered night-time data (Oikawa et al., 2017). CLM-Palm struggled to represent daily average NEE during the non-haze drought and haze drought periods, most likely due to the models' soil water stress function (Sellers et al., 1986) and missing plant hydraulic processes in the overarching CLM4.5 (Oleson et al., 2013). Therefore, we decided to solely focus on NEE to describe the overall CO<sub>2</sub> flux behaviour of the oil palm plantation during the extreme events of drought and haze. However, we used the night-time NEE (i.e., respiration) as a proxy for the overall behaviour of oil palm monoculture respiration and disentangled its driving climatic variables. Seasonal differences in  $u^*$ , especially during night-time, might impact the performance of eddy covariance gap filling. However, we found no significant differences ( $P < 0.05$ ) in  $u^*$ , which could have affected the proportion of available night-time data during the different meteorological periods. Therefore, we consider the applied gap filling procedure and derived flux averaging as robust and representative for the studied time periods.

In this study, we assign H, LE and NEE as positive when they are directed away from the surface. To avoid negative values of  $A_{\text{max}}$  and for better readability, we perform sign

conversion of  $A_{\text{max}}$ . All statistical analyses and graphing were performed with R version 3.1.1 (R Core Development team, 2014).

## 2.5 Multiple linear regression model

We used a multiple linear regression model (MLRM) (Whittingham et al., 2006; Ray-Mukherjee et al., 2014) to investigate the temporal contribution of climatic variables to observed trends in NEE. The first MLRM used in this study considers the diel-averaged NEE, which includes both the photosynthetic and respiratory processes. We built the model to include vapour pressure deficit (VPD), atmospheric CO<sub>2</sub> concentration (CO<sub>2</sub>), fraction of diffuse radiation (fdifRad), wind speed (wind), air temperature (tair) and actual evapotranspiration divided by potential evapotranspiration (ET\_ET\_pot). Unless otherwise stated, the environmental variables used in this study are measured above the canopy in 22 m height. The form of the model for the 24 h averaged NEE is as follows:

$$\text{NEE} = \beta_1 \text{VPD} + \beta_2 \text{CO}_2 + \beta_3 \text{fdifRad} + \beta_4 \text{wind} + \beta_5 \text{tair} + \beta_6 \text{ET\_ET\_pot}, \quad (1)$$

where  $\beta$  is the slope. The MLRM parameters were estimated using the ordinary least-squares method. We transformed each parameter by subtracting the mean and dividing it by the standard deviation. The transformed data have a mean zero with a standard deviation of 1. In the case of the transformed data, as well as when an intercept was added in the 24 h original NEE model, temperature and VPD became insignificant ( $p$  value  $> 0.5$ ), and thus the goodness of fit decreased by 53 %. Therefore, we did not include the intercept term in Eq. (1) because without the intercept the model gave a relatively high goodness of fit (see Supplement, Tables S1 and S2). Initially, we included more parameters for the MLRM since we did not put a limit on the number of covariates to explain the observed NEE. However, we applied different case scenarios where we examined different MLRMs in relation to setting up the model (see sample model case scenarios in the Supplement, Table S2). In these case scenarios we included Akaike information criterion (AIC) scores along with the goodness of fit values to ensure the following model criteria: (a) the  $\beta$  is highly statistically significant (Chatfield, 1995), (b) the predictors are chosen in such a way so that they are least correlated (Zuur et al., 2010) and (c) the model has high AIC score. In the initial model setup (Eq. 1) we included drought indicators such as precipitation and soil moisture at different depths but these predictors were not significant ( $p$  value  $> 0.1$ ). Thus, we excluded them from the model and used only predictors which were highly significant. We also standardised the data to consider normality and non-linearity (Z. Chen et al., 2018), but these changes reduced the goodness of fit by a large amount. Therefore, throughout this study we use the data in the original form.

For the second MLRM, we focused on the midday NEE (10:00–14:00 LT), which is dominated by photosynthesis and thus avoids any issues of night-time flux uncertainties. In this case, we used predictors for our model which were significant, i.e. incoming photosynthetically active radiation (PAR<sub>in</sub>), tair, VPD, CO<sub>2</sub> and fdifRad. The form of the model for the daytime NEE is as follows:

$$\text{NEE} = \beta_1 \text{PAR}_{in} + \beta_2 \text{tair} + \beta_3 \text{VPD} + \beta_4 \text{CO}_2 + \beta_5 \text{fdifRad} + \beta_6 \text{ET\_ET\_pot} \quad (2)$$

To complement daytime NEE, we also looked at night-time NEE (19:00–05:30 LT). The modelled NEE for night-time takes the following form:

$$\text{NEE} = \beta_1 \text{tair} + \beta_2 \text{VPD} + \beta_3 \text{ET\_ET\_pot} + \beta_4 \text{tair}_{12} + \beta_5 \text{wind} \quad (3)$$

For the night-time NEE, we also considered environmental variables within the canopy profile, i.e. air temperature measured at 12 m above the soil (tair<sub>12</sub>). At night, soil respiration could be influenced by this environmental factor (Zhou et al., 2013). Initially, we also tested the model using soil temperature and soil moisture but these parameters were not significant.

### 2.5.1 NEE under intensified drought and haze conditions

We used the above three NEE models (Eqs. 1 to 3) based on the 2015 drought and haze conditions to investigate the impacts of intensified non-haze drought (NHD+) and haze drought (HD+) conditions on oil palm NEE. These two scenarios focus on the response of oil palm to short-term more extreme atmospheric conditions associated with projected more severe future ENSO events during the current life cycle of the oil palm plantation, which was planted 1999–2004 and is therefore in a mature stage and in the middle of its life cycle. The temperature change in the scenarios, however, only reflects short-term extreme conditions and does not consider slow long-term effects of a changing climate.

Under intensified non-haze drought (NHD+) during the current rotation cycle of the oil palm plantation, we assume a short-term increase in VPD, incoming PAR and air temperature and a decrease in diffuse radiation. Thus, we modified the mean of the model input variables as VPD +20%, fdifRad –20%, tair +20%, PAR<sub>in</sub> +20%, ET\_ET\_pot –20% and tair<sub>1</sub> +20%. Under intensified haze drought (HD+) we modified the mean of the environmental variables (VPD by +20%, CO<sub>2</sub> by +20%, fdifRad by +20%, tair by +20%, PAR<sub>in</sub> by –20%, ET\_ET\_pot –20% and tair<sub>12</sub> by +20%) in the model. For both scenarios (NHD+ and HD+), however, we kept the coefficients of the input parameters constant.

## 3 Results

### 3.1 Atmospheric and environmental conditions

Strong inter-seasonal differences in precipitation patterns, air temperature and atmospheric VPD characterise the study period, with the year 2015 being slightly drier and warmer as during the reference periods of 2014 and 2016 (Table 1). From March 2015, both the daily mean air temperature and daily mean VPD showed a steady increase and reached their maxima during the haze drought period in mid-October (Fig. 2). The first 4 months in 2015 were cooler and wetter than during the reference period (Table 1). From May until mid-September, when the non-haze drought hit the area in 2015, air temperature and VPD were of similar magnitudes in 2015 and the reference period but accumulated precipitation was as little as 192 mm in 2015 compared to 594 mm during the reference period (Supplement, Fig. S1). Inter-seasonal differences in air temperature and in VPD were most pronounced from mid-September until mid-November, when haze covered the area in 2015. During that time, mean air temperature was  $28.3 \pm 0.8$  °C and mean VPD was  $8.71 \pm 2.57$  hPa, which is 2.3 °C and 4.98 hPa higher than during the reference period. There were sharp contrasts in soil water content (SWC) in 2015 between the pre-drought and haze drought period due to the absence of precipitation in the latter period. SWC in the upper two soil layers (30 and 60 cm) declined by 35%, respectively, while in the bottom layer (100 cm) the decline was 10% (Table 1). During the reference period, differences in SWC were less pronounced, with a maximum decline of 26% in the upper two soil layers. Daily mean global radiation and daily mean incoming photosynthetically active radiation (PAR) showed strong periodical and day-to-day variations over the course of the study period. In 2015, irradiance reached its maximum during the non-haze drought period in late July and mid-August (Fig. 2). After this peak, the continuous emergence of haze led to a substantial decrease in both R<sub>G</sub> and PAR (Table 1). Simultaneously, fraction of diffuse radiation increased from 0.21 to 0.99 and diffuse radiation remained almost the sole short-wave radiation component for almost 2 months. Compared to the reference period, daily average incoming PAR during the haze drought in 2015 decreased by  $107 \mu\text{mol m}^{-2} \text{s}^{-1}$  (–36%), while the fraction of diffuse radiation increased by 0.12 (13%) (Table 1). The persistence and density of the haze in 2015 is reflected in daily average sunshine duration (Table 1). During the haze drought period, the sun was, on average, visible for  $50 \text{ min d}^{-1}$ , which is equal to 7% within 12 h of potential daylight (sun above the horizon). During the pre-drought, non-haze drought and post-haze period, the sun was visible for 6.7 (56%), 10 (83%) and 6 (50%) h d<sup>–1</sup>, respectively. Atmospheric CO<sub>2</sub> concentration during the haze drought and post-haze period in 2015 was 5% (20 ppm) and 6% (24 ppm) higher than during the reference period.

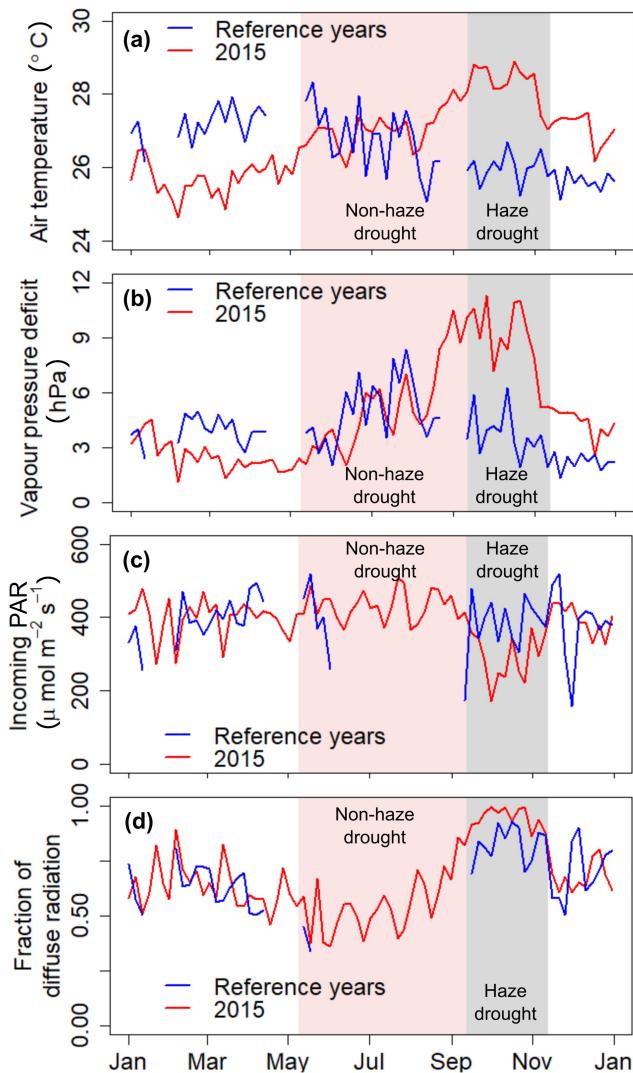


**Figure 2.** The 5 d running mean of air temperature (a), atmospheric vapour pressure deficit (VPD) (b), incoming photosynthetically active radiation (PAR) (c) and fraction of diffuse radiation (d) during 2015 and the reference time period. Shaded areas in red and grey mark the non-haze drought and the haze drought periods in 2015, respectively.

### 3.2 Net ecosystem CO<sub>2</sub> exchange, carbon accumulation and yield

The oil palm plantation was a net sink of CO<sub>2</sub> during the study period. Mainly due to the impact of the haze period, net ecosystem CO<sub>2</sub> exchange (NEE) in 2015 ( $-1.79 \pm 13.53 \mu\text{mol m}^{-2} \text{s}^{-1}$ ) was significantly weaker ( $P < 0.01$ ) compared to the reference period ( $-2.20 \pm 14.48 \mu\text{mol m}^{-2} \text{s}^{-1}$ ) (Table 2). NEE was higher compared to the reference period (Fig. 3) and CO<sub>2</sub> uptake showed a slight increase coinciding with the drought-related increase in incoming PAR only in the very beginning of 2015 and during the period June–September 2015. The beginning of the haze

drought marks a strong transition where CO<sub>2</sub> uptake initially decreased with developing haze, followed by a 2-month period where the oil palm plantation turned into a small source of CO<sub>2</sub> to the atmosphere.

Carbon accumulation by the oil palm plantation was relatively strong in the first months of 2015 and exceeded accumulation of the reference period by up to  $80 \text{ g C m}^{-2}$  (Fig. 3b). During the following months until mid-June, carbon accumulation of the reference period surpassed 2015 carbon accumulation, but by mid-August these differences were offset. Due to the haze from October to mid-November 2015, carbon accumulation initially paused, followed by small overall carbon loss of  $10 \text{ g C m}^{-2}$  within 40 d. After the haze, the oil palm plantation was not able to offset the pause in carbon accumulation and carbon losses during the haze and therefore the total amount of accumulated carbon in 2015 was  $152.7 \text{ g C m}^{-2}$  (18 %) lower compared to the reference period (Table 1).

Over the course of the non-haze drought, the oil palm plantation reduced its maximum rate of photosynthesis ( $A_{\text{max}}$ ) (Fig. 4). However, drought-related changes in meteorological and environmental conditions caused a minor (3 %) decrease in  $A_{\text{max}}$  compared to pre-drought conditions. With the continuous development of haze in September 2015 and related absence of direct sunlight, the oil palm plantation seemed to compensate for the overall haze-related reduction in incoming PAR, with a jump of  $A_{\text{max}}$  by  $13 \mu\text{mol m}^{-2} \text{s}^{-1}$  (37 %) within a couple of days (Fig. 4). This compensation effect of relatively high  $A_{\text{max}}$  continued over the haze drought period, with  $A_{\text{max}}$  being  $4.8 \mu\text{mol m}^{-2} \text{s}^{-1}$  (18 %) higher than during the non-haze drought.

Using linear regression between monthly NEE and oil palm yield, we found that a 6-month delay in yield showed highest  $R^2$  of 0.36 ( $P < 0.01$ ) with NEE. Therefore, we consider the period November 2015 to May 2016 as the time when NEE and carbon accumulation during the non-haze drought and haze drought in 2015 were reflected in monthly oil palm yield. From August 2015, monthly oil palm yield declined continuously from  $3.93 \text{ t ha}^{-1}$  to its minimum of  $1.05 \text{ t ha}^{-1}$  in May 2016. Compared to the same period (November–May) in the 2 years before and the year after the ENSO event, average yield affected by 2015 drought and haze was 32 % ( $0.70 \text{ t ha}^{-1}$ ) lower. Considering the 2015 haze drought only, average oil palm yield 6–9 months after the beginning of the haze drought was even 50 % ( $1.1 \text{ t ha}^{-1}$ ) lower compared to the non-ENSO years.

### 3.3 Evapotranspiration and turbulent heat fluxes

Total evapotranspiration (ET) derived from EC latent heat flux (LE) measurements was  $1245 \pm 362 \text{ mm yr}^{-1}$  in 2015 and  $1580 \pm 469 \text{ mm yr}^{-1}$  during the reference period (Table 2), with a higher share of ET on precipitation during the reference period (77.9 %) compared to 2015 (64.5 %). During the non-haze drought and haze drought periods, the oil

**Table 1.** Meteorological parameters (daily mean  $\pm$ SD, or accumulated for precipitation and carbon) derived from 30 min averages or sums during the pre-drought, non-haze drought, haze drought and post-haze periods in 2015; for the entire year 2015; and the reference period (May 2014–December 2014, January 2016–July 2016).

Period	Air temperature [°C]	Precipitation [mm]	Vapour pressure deficit (VPD) [hPa]	Soil moisture, 30 cm depth [vol %]	Soil moisture, 60 cm depth [vol %]	Soil moisture, 100 cm depth [vol %]	Incoming PAR [ $\mu\text{mol m}^{-2} \text{s}^{-1}$ ]	Fraction of diffuse radiation	Sunshine duration [ $\text{h d}^{-1}$ ]
Pre-drought (128 d)	25.7 $\pm$ 0.7	1003	2.53 $\pm$ 1.25	32.5 $\pm$ 1.8	31.9 $\pm$ 1.4	32.3 $\pm$ 0.8	396.9 $\pm$ 105.0	0.67 $\pm$ 0.19	6.7 $\pm$ 6.9
Drought (127 d)	27.1 $\pm$ 0.7	192	5.30 $\pm$ 2.60	27.9 $\pm$ 4.3 <sup>a</sup>	26.8 $\pm$ 4.3 <sup>b</sup>	27.1 $\pm$ 2.9	432.0 $\pm$ 70.6	0.57 $\pm$ 0.18	10.0 $\pm$ 7.1
Haze (61 d)	28.3 $\pm$ 0.8	127	8.71 $\pm$ 2.57	18.1 $\pm$ 1.5	17.5 $\pm$ 0.2	24.4 $\pm$ 0.1	293.2 $\pm$ 97.3	0.95 $\pm$ 0.07	0.8 $\pm$ 3.2
Post-haze (49 d)	27.1 $\pm$ 0.9	608	4.30 $\pm$ 1.45	23.4 $\pm$ 1.3 <sup>c</sup>	20.6 $\pm$ 1.9 <sup>c</sup>	26.8 $\pm$ 2.1	393.8 $\pm$ 111.0	0.71 $\pm$ 0.17	6.0 $\pm$ 6.8
2015	26.8 $\pm$ 1.2	1930	4.76 $\pm$ 2.96	27.2 $\pm$ 6.1	26.4 $\pm$ 6.2	28.4 $\pm$ 3.6	391.4 $\pm$ 104.7	0.69 $\pm$ 0.21	6.8 $\pm$ 7.2
Reference period	26.5 $\pm$ 1.1 <sup>d</sup>	2030	4.0 $\pm$ 2.0 <sup>d</sup>	28.3 $\pm$ 1.7 <sup>e</sup>	29.9 $\pm$ 1.8 <sup>f</sup>	25.5 $\pm$ 2.0 <sup>e</sup>	397.6 $\pm$ 103.6 <sup>g</sup>	–	–

<sup>a</sup> no data 26.07.–06.09.2015. <sup>b</sup> no data 05.08.–06.09.2015. <sup>c</sup> no data 14.12.–31.12.2015. <sup>d</sup> no data 30.08.–09.09.2014, 12.01.–04.02.2016, 14.04.–11.05.2016. <sup>e</sup> no data 31.05.–10.09.2014, 01.01.–04.02.2016, 14.04.–11.05.2016. <sup>f</sup> no data 31.05.–10.09.2014, 01.01.–11.02.2016, 14.04.–11.05.2016. <sup>g</sup> no data 31.05.–08.09.2014, 12.01.–04.02.2016, 14.04.–11.05.2016.

**Table 2.** Net CO<sub>2</sub> flux, maximum rate of photosynthesis ( $A_{\text{max}}$ ), accumulated carbon, atmospheric CO<sub>2</sub> concentration, Bowen ratio, evapotranspiration (ET) and actual ET divided by potential ET ( $\text{ET} / \text{ET}_{\text{pot}}$ ) (daily mean  $\pm$ SD, or accumulated for precipitation and carbon) derived from 30 min averages or the daily average ( $A_{\text{max}}$ , Bowen ratio) during the pre-drought, non-haze drought, haze drought and post-haze periods in 2015; the entire year 2015; and the reference periods of May 2014–December 2014 and January 2016–July 2016.

Period	Net CO <sub>2</sub> flux (net ecosystem exchange) [ $\mu\text{mol m}^{-2} \text{s}^{-1}$ ]	Maximum rate of photosynthesis ( $A_{\text{max}}$ ) [ $\mu\text{mol m}^{-2} \text{s}^{-1}$ ]	Accumulated carbon [ $\text{g C m}^{-2}$ ]	CO <sub>2</sub> concentration [ppm]	Bowen ratio	Evapotranspiration (ET) ( $\text{mm d}^{-1}$ )	$\text{ET} / \text{ET}_{\text{pot}}$
Pre-drought (128 d)	−2.10 $\pm$ 12.91	27.4 $\pm$ 8.1	278.6 $\pm$ 81.8	416 $\pm$ 29	0.12 $\pm$ 0.10	3.6 $\pm$ 4.9	0.55 $\pm$ 0.11
Drought (127 d)	−2.33 $\pm$ 14.07	26.6 $\pm$ 5.1	306.8 $\pm$ 91.1	412 $\pm$ 25	0.13 $\pm$ 0.13	3.7 $\pm$ 4.8	0.45 $\pm$ 0.09
Haze (61 d)	−0.33 $\pm$ 12.70	31.4 $\pm$ 8.3	23.0 $\pm$ 5.5	429 $\pm$ 26	0.16 $\pm$ 0.14	2.5 $\pm$ 3.5	0.45 $\pm$ 0.07
Post-haze (49 d)	−1.41 $\pm$ 14.50	29.1 $\pm$ 6.6	69.1 $\pm$ 20.0	429 $\pm$ 29	0.14 $\pm$ 0.14	3.4 $\pm$ 4.6	0.48 $\pm$ 0.11
2015	−1.79 $\pm$ 13.53	28.0 $\pm$ 7.2	676.6 $\pm$ 199.2	418 $\pm$ 28	0.13 $\pm$ 0.12	3.4 $\pm$ 4.6	0.49 $\pm$ 0.11
Reference period	−2.20 $\pm$ 14.48	31.8 $\pm$ 8.4 <sup>a</sup>	829.3 $\pm$ 242.3	407 $\pm$ 30	0.09 $\pm$ 0.05	4.3 $\pm$ 5.5	0.59 $\pm$ 0.15

<sup>a</sup> no data 31.05.–08.09.2014, 12.01.–04.02.2016, 14.04.–11.05.2016.

palm plantation experienced strong water loss from ET as ET was 2.5 and 1.2 times the amount of precipitation, respectively. ET was lowest during the haze drought period (Fig. 5, Table 2), mainly driven by the reduction in incoming solar radiation and PAR as well as by oil palm drought and heat stress, which may have triggered partial stomata closure, especially in the beginning of the haze drought when VPD was high (Fig. 2). Conversely, partial stomata closure during high VPD, as well as the absence of precipitation and related drying of the upper soil, generally increased sensible heat fluxes (H) at the cost of LE and ET, reflected in the behaviour of the Bowen ratio (H/LE) (Fig. 5). From the first half of the pre-drought period into the second half of the non-haze pe-

riod, the Bowen ratio showed a steady but relatively small decline. However, the end of the non-haze drought and the beginning of the haze drought period mark a strong transition in the behaviour of the Bowen ratio, manifested by a strong jump, peak values of  $\sim$ 0.38 and average of 0.25 for approx. 1 month. This jump in the Bowen ratio might be related to the increasing density of the haze and related reduction in incoming PAR in combination with high VPD which decrease LE mainly via oil palm water and light stress to a greater extent than the general drying of the soil and lack of precipitation.

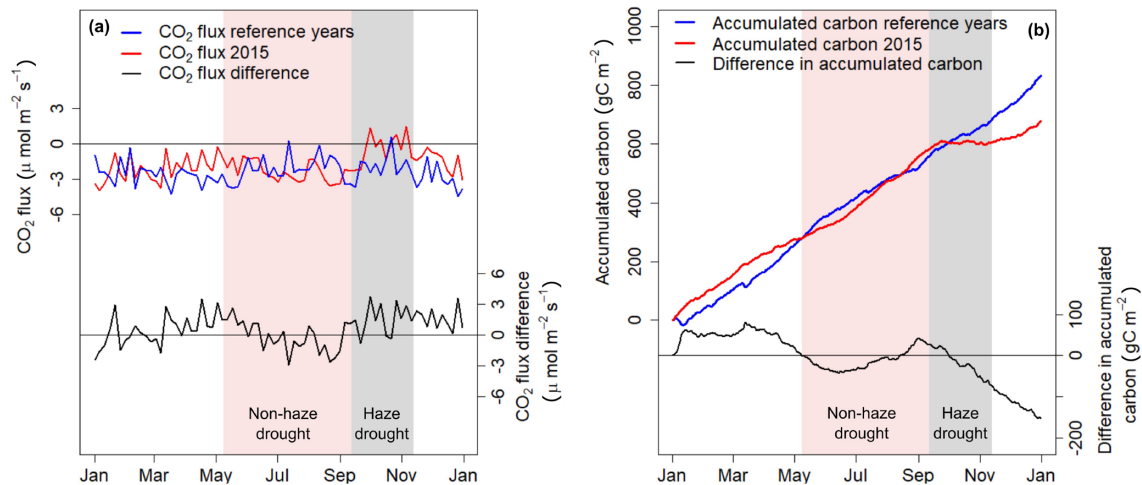


**Figure 3.** (a) The 5 d running mean of net ecosystem CO<sub>2</sub> exchange (NEE) during 2015 and the reference time period and 5 d running mean of CO<sub>2</sub> flux difference (2015 minus reference time period). (b) Accumulated carbon uptake derived from CO<sub>2</sub> fluxes during the period 2015 and the reference time period and differences in accumulated carbon between the two periods (2015 minus reference time period). Shaded areas in red and grey mark the non-haze drought and the haze drought period in 2015, respectively.

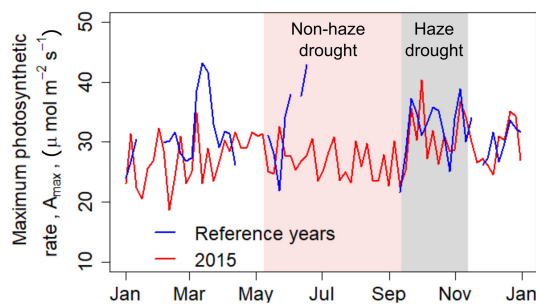


**Figure 4.** The 5 d running mean of maximum rate of photosynthesis ( $A_{\max}$ ) during 2015 and during the reference time period. Sign convention has been performed to avoid negative values of  $A_{\max}$ . Shaded areas in red and grey mark the non-haze drought and the haze drought period in 2015, respectively.

### 3.4 Drivers of net ecosystem CO<sub>2</sub> exchange

Modelled NEE from our MLRM simulated a small positive effect on NEE during the non-haze drought, with an increase in CO<sub>2</sub> uptake by  $0.32 \mu\text{mol m}^{-2} \text{s}^{-1}$ , and a negative effect on NEE during the haze drought, with a decrease in CO<sub>2</sub> uptake by  $0.99 \mu\text{mol m}^{-2} \text{s}^{-1}$  (Fig. 6, Supplement Table S5). Modelled NEE is in good agreement with the measured NEE, i.e. at midday (10:00–14:00 LT), at night-time (19:00–05:30 LT) and for average NEE (00:00–24:00 LT) the model explains 98 %, 94 % and 83 %, respectively, of the temporal variability in the measured NEE. Overall, the relative change of meteorological and environmental parameters during the non-haze drought and haze drought caused a more pronounced response of NEE in the latter period compared to

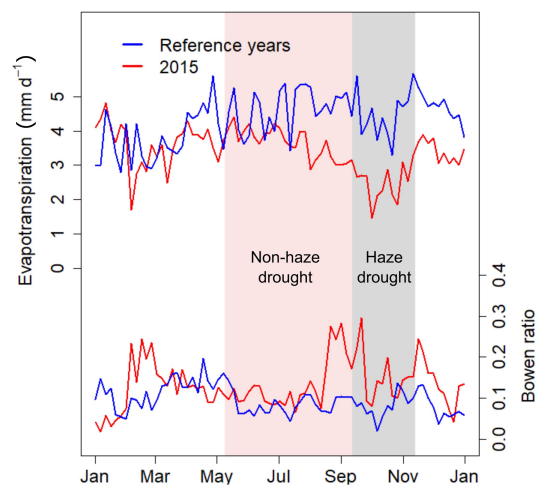


**Figure 5.** The 5 d running mean of daily evapotranspiration and ratio of sensible to latent heat fluxes (Bowen ratio) during 2015 and the reference time period. Shaded areas in red and grey mark the non-haze drought and the haze drought period in 2015, respectively.

non-drought and non-haze conditions, especially during midday (Fig. 6).

During the non-haze drought, changes in radiation components were the main predictors of changes in midday NEE. Higher incoming PAR increased CO<sub>2</sub> uptake, while at the same time this gain in CO<sub>2</sub> uptake was compensated for by the negative impact of decreasing fraction of diffuse radiation (Fig. 6, Supplement Table S5). However, this estimated effect of the changes in irradiance on NEE was clearly small compared to the negative effects of dim light conditions during the haze drought where a reduction in incoming PAR re-

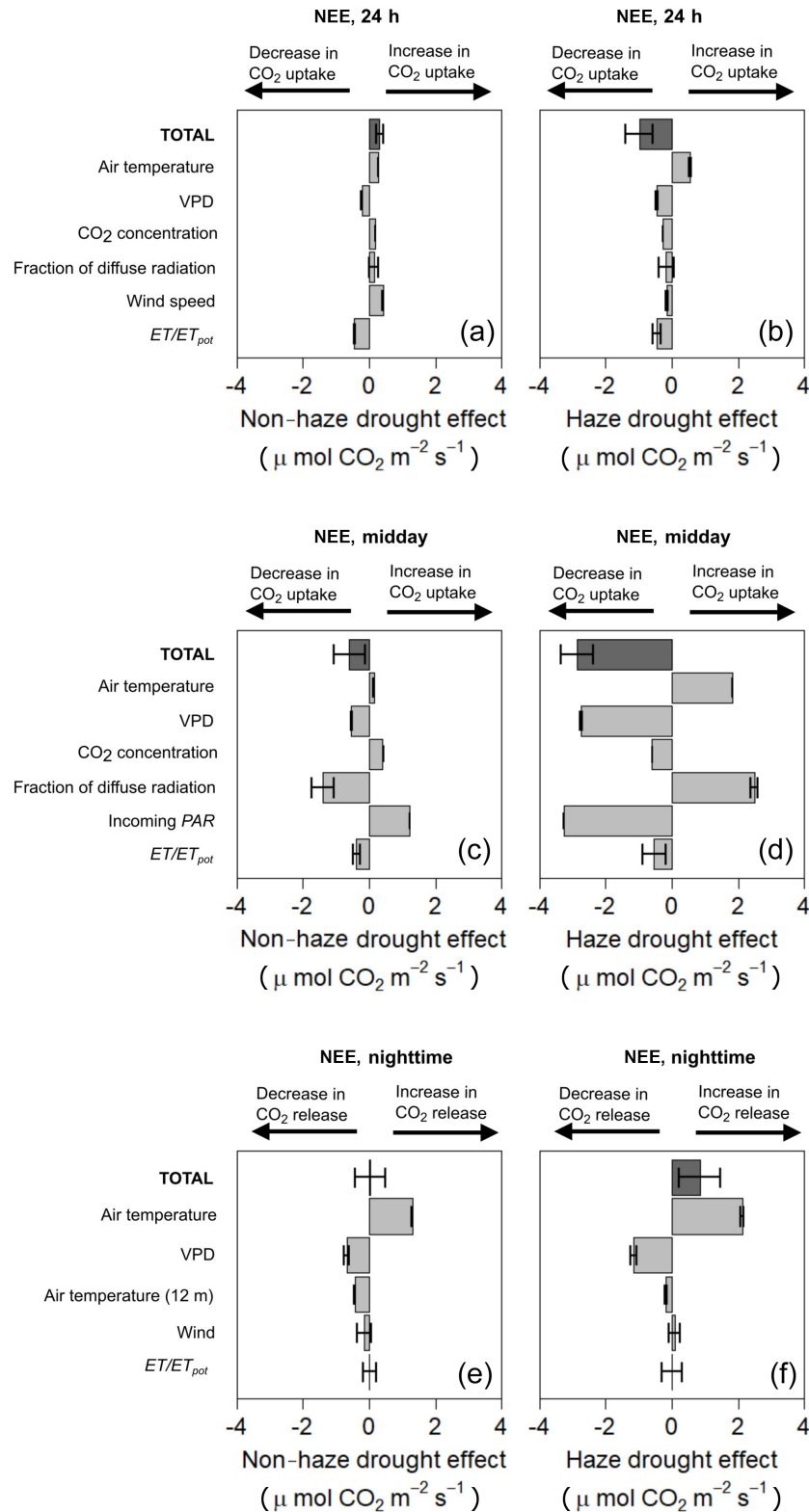


**Figure 6.** Contribution and effect of meteorological and environmental parameters during the non-haze drought and haze drought period on the 24 h (a, b), midday (c, d) and night-time (e, f) net ecosystem CO<sub>2</sub> exchange (NEE) compared to non-drought and non-haze conditions using a multiple linear regression model (MLRM). Error bars show the standard error.

sulted in a strong decrease in CO<sub>2</sub> uptake (Fig. 6). Further, the effect of incoming PAR and fraction of diffuse radiation in midday NEE was reversed during the haze drought compared to the non-haze drought and the decrease in fraction of diffuse radiation contributed to higher midday CO<sub>2</sub> uptake but these positive effects were almost offset completely by the decrease in incoming PAR.

Increasing VPD had a negative impact on midday NEE (decrease in CO<sub>2</sub> uptake), while the increase in air temperature had a positive impact on midday NEE (increase in CO<sub>2</sub> uptake). Oil palm drought stress, manifested in a general decrease in ET/ET<sub>pot</sub> (Table 2), was less severe during the non-haze drought compared to the haze drought period, resulting in a slightly more pronounced decrease in CO<sub>2</sub> uptake during the latter period (Fig. 6). The observed changes in atmospheric CO<sub>2</sub> concentrations during the non-haze drought and haze drought suggest that the oil palm might respond via photosynthesis and stomata behaviour to the elevated atmospheric CO<sub>2</sub> levels. However, rising atmospheric CO<sub>2</sub> concentration had no fertilisation effect for the oil palm plantation, on the contrary, the increase in CO<sub>2</sub> concentration contributed to a decrease in CO<sub>2</sub> uptake (Fig. 6).

During both non-haze drought and haze drought, the change in night-time (19:00–05:30 LT) air temperature above the canopy was the main predictor of changes in night-time NEE (respiration). The increase in air temperature tended to increase respiration. This was more pronounced during the haze drought compared to the non-haze drought (Fig. 6, Supplement Table S5 and S6).

### 3.5 NEE under intensified drought and haze conditions

Our two model projections, where we increased the effects of non-haze drought and haze drought conditions based on the 2015 drought and haze conditions, showed that increased non-haze drought conditions (NHD+) enhanced CO<sub>2</sub> uptake, while increased haze drought (HD+) weakened CO<sub>2</sub> uptake and might even promote CO<sub>2</sub> release (Fig. 7, Supplement Table S7). Daily average (24 h) CO<sub>2</sub> uptake in NHD+ was increased by 2.25 μmol m<sup>-2</sup> s<sup>-1</sup> compared to the 2015 non-haze drought conditions. NHD+ might enhance midday CO<sub>2</sub> uptake and night-time respiration, which increased by 6.52 and 1.59 μmol m<sup>-2</sup> s<sup>-1</sup>, respectively, mainly due to the effect of a high air temperature in NHD+, which is also the main predictor of daily average, midday and night-time NEE (Supplement Table S7). Incoming PAR is the dominant light parameter for NEE and increases in incoming PAR in NHD+ are able to offset the modelled negative impact of decreased fraction of diffuse radiation on NEE. This is contrary to what the model suggested for the 2015 non-haze drought reference conditions, where we observe that the increase in incoming PAR was not able to offset the negative impacts on NEE due to decreased fraction of diffuse radiation. Similar to NHD+, air temperature in the increased haze drought scenario (HD+) was the main predictor

of NEE and contributed to a high midday and daily average (24 h) CO<sub>2</sub> uptake and also to a high night-time respiration (Fig. 7, Supplement, Table S8). However, the negative effects of HD+ offset the positive effects of increased air temperature. Daily average (24 h) CO<sub>2</sub> uptake and midday CO<sub>2</sub> uptake in HD+ were decreased by 0.85, 4.51 μmol m<sup>-2</sup> s<sup>-1</sup>, respectively, while night-time ecosystem respiration was increased by 2.53 μmol m<sup>-2</sup> s<sup>-1</sup>. Incoming PAR in HD+ remains the dominant light parameter on midday NEE and its decrease cannot be offset by the positive effects of increased fraction of diffuse radiation. In HD+, midday VPD is of less relative importance on NEE compared to the reference haze drought conditions. As already observed in the 2015 haze drought model output, increased CO<sub>2</sub> concentration in HD+ does not act as an additional fertilisation for the oil palm plantation. In contrast, the negative impact of increased CO<sub>2</sub> concentration on NEE becomes the dominant predictor of NEE in HD+. Our two scenarios indicate that increased drought stress, reflected by decreasing ET/ET<sub>pot</sub>, has a more pronounced negative impact on NEE in HD+ compared to NHD+. However, oil palm seems to be relatively resistant against drought since the overall impact of changes in ET/ET<sub>pot</sub> on NEE was relatively small in both scenarios.

## 4 Discussion

### 4.1 Oil palm response to drought and haze conditions

Oil palm has exceptionally high photosynthetic efficiency compared to most vascular plants (Apichatmeta et al., 2017) but this efficiency comes with a downside: oil palm, like many other tropical plants, shows a distinct reaction to changes in atmospheric and soil parameters, with gradual symptoms of water and heat stress that directly affect photosynthesis and evapotranspiration as well as fruit bunch development and yield (Bakoumé et al., 2013; Paterson et al., 2013). During our study period, we observed that accumulated annual precipitation in 2015 and during the reference period was on the lower limit of reported optimum precipitation range for oil palm (Pirker et al., 2016). However, oil palm requires a minimum precipitation of 100 mm month<sup>-1</sup> to avoid drought stress (Corley and Tinker, 2016). This was not fulfilled in September 2014, from June to October 2015 or in January 2016. Previous studies report a strong correlation between NEE and soil moisture (Méndez et al., 2012; Cha-um et al., 2013), with declining CO<sub>2</sub> assimilation under dry conditions. In our study, however, we found no strong correlation between NEE and soil moisture conditions or between NEE and ET/ET<sub>pot</sub> during the non-haze drought and haze drought period. This might be explained by the relatively stable soil moisture conditions in deeper layers (100 cm) of the oil palm plantation which, compared to the upper layers (30 and 60 cm) showed only a moderate de-

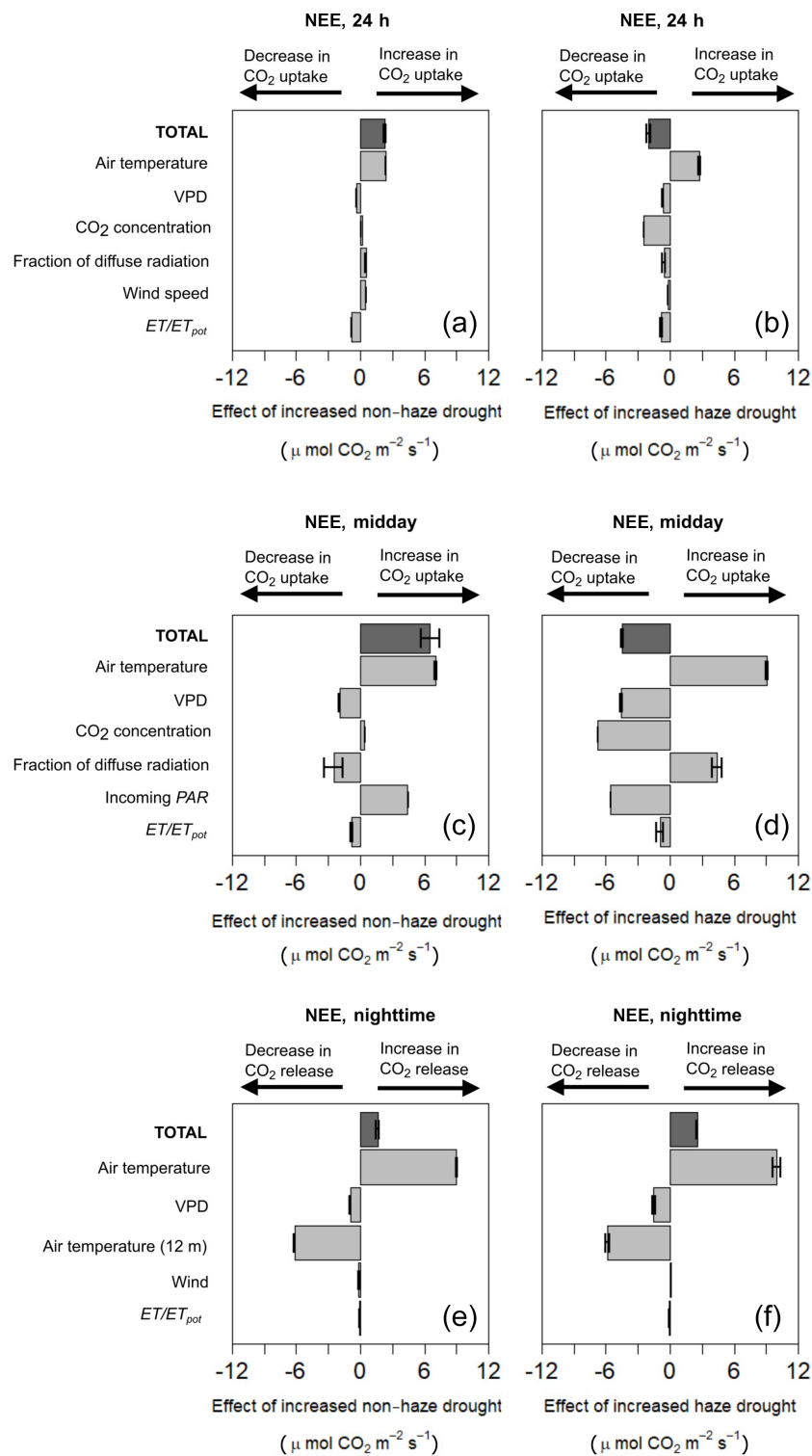


**Figure 7.** Contribution and effect of meteorological and environmental parameters considering increased non-haze drought (NHD+) and increased haze drought (HD+) scenario on the 24 h (a, b), midday (c, d) and night-time (e, f) net ecosystem CO<sub>2</sub> exchange (NEE) using a multiple linear regression model (MLRM). Error bars show the standard error.

crease during both non-haze drought and haze drought (Table 1). Oil palm seems to be able to uptake water from deep soil and store the water in the trunk during night, supporting water use during peak hours of photosynthesis (Niu et al., 2015; Meijide et al., 2017). Therefore, the relatively moderate decrease in soil moisture in deeper soil layers might have had a limited effect on NEE.

Temperature increase and related heat stress is another factor that might negatively affect the growth of oil palm (Oettli et al., 2018). Our analysis did not support this finding because during the non-haze drought the effect of increasing temperature on NEE was almost negligible. During the haze drought, higher air temperature had a positive impact on CO<sub>2</sub> uptake, although the haze period experienced the highest air temperature during the entire study period. Changes in temperature and moisture availability also impact oil palm ecosystem respiration. Matysek et al. (2018) observed high heterotrophic carbon loss from drained peat soils in a Malaysian oil palm plantation during the dry season and Sigau and Hamid (2018) found similar behaviour in Malaysian rubber and oil palm plantations on drying Haplic Nitisols soils but both studies report only a minor impact from increased soil temperature on soil respiration. Autotrophic respiration, however, tends to decrease with increasing leaf temperature (Slot et al., 2014). In our study, the increase in air temperature tended to increase night-time ecosystem respiration and therefore might also lead to higher daytime respiration during the non-haze drought and haze drought period.

Oil palm, similar to other tropical plant species, seems particularly susceptible to changes in atmospheric VPD (Dufrene and Saugier, 1993; Henson, 2000; Cunningham, 2005; Lamade and Bouillet, 2005; Wahid et al., 2005; Bayona-Rodríguez and Romero, 2016; Mathews and Ardiyanto, 2016) with high levels of VPD causing partial closure of stomata and limiting photosynthesis and transpiration. Our MLRM and measurements are in line with these findings and high levels of VPD had a stronger impact on NEE during the haze drought period compared to the non-haze drought period. To a certain extent, oil palm is capable of adjusting its stomatal regulation to short-term periods of moderate VPD and soil water deficit by increasing its maximum rate of photosynthesis ( $A_{\max}$ ) (Dufrene and Saugier, 1993; Apichatmeta et al., 2017). However, during the non-haze drought and haze drought those two environmental parameters exerted only a minor impact on  $A_{\max}$  and changes in irradiance seemed to be the dominant driver of  $A_{\max}$ .

Oil palm grows in regions with high solar flux densities (Barcelos et al., 2015) and it is able to strategically optimise its photosynthesis to light conditions, with pronounced diurnal effects and maximum efficiency before or at about midday (Apichatmeta et al., 2017). In our study, measurements and MLRM results showed strongest response of oil palm NEE to drought, haze and changes in irradiance during midday. Due to the reduction of incoming PAR for al-

most 2 months, the haze was a major and persistent disturbing factor for oil palm NEE and  $A_{\max}$ . The initial increase in diffuse light conditions and its positive impact on  $A_{\max}$  and NEE cannot compensate for the reduction in incoming PAR. Therefore, the observed pause in carbon accumulation and even small carbon release during the haze drought could have been prevented, since without the haze, the oil palm plantation would have remained a sink of CO<sub>2</sub> during that period.

Changes in oil palm yield are one direct consequence of varying nutrient, meteorological and climatic conditions (Sun et al., 2011; Mathews and Ardiyanto, 2016; Oettli et al., 2018). Prolonged drought and nutrient limitation not only affect carbon accumulation via photosynthesis but leads to abortion of female inflorescences and failing bunch yield (Bakoumé et al., 2013). In an oil palm plantation in Central Kalimantan (Indonesia) dense haze from peat fires resulted in poor quality of fruit bunches and low oil palm extraction rates (Mathews and Ardiyanto, 2016). Fertilisation under water stress conditions has a negative impact on oil palm growth and may further reduce oil palm yield while fertilisation during well-watered conditions promotes oil palm growth and yield (Sun et al., 2011). At our study site, fertilisers are applied at the end of the wet season (April–May), and in 2015 precipitation was still sufficiently high to maintain well-watered soil conditions during the fertilisation. Oil palm yield in 2016, and its initial sharp drop by the end of 2015, can therefore be related to the drought and haze conditions and the haze was the driving stressor. Similar to the effects of haze on NEE, without the haze oil palm yield might not have experienced such a sharp decline.

Short-term elevated CO<sub>2</sub> exposure on oil palm seedlings (Ibrahim et al., 2010; Jaafar and Ibrahim, 2012) and on mature oil palm (Henson and Harun, 2005a, b) have shown that elevated CO<sub>2</sub> concentrations promote plant growth, due to elevated rates of photosynthesis and reduced water loss by transpiration. To our knowledge, no comprehensive study has investigated the complex interplay of elevated CO<sub>2</sub> concentrations, increased temperature and decrease in radiation in oil palm. Mathews and Ardiyanto (2016) speculate that short-term elevated levels of CO<sub>2</sub> under haze conditions and related potentially strong stomatal opening may offset the lack of irradiance and related shorter timing of stomatal opening. Based on leaf–gas exchange measurements in trees, Urban et al. (2014) come to a contradiction that low irradiance is incapable of activating stomatal opening since plants exposed to elevated CO<sub>2</sub> levels require higher stomatal activation energy. From our results, it is highly doubtful that elevated CO<sub>2</sub> exposure during the haze had any fertilisation effect. On the contrary, increasing atmospheric CO<sub>2</sub> concentration acted as an additional stress factor for oil palm and decreased CO<sub>2</sub> uptake.

Ground-level ozone exerts strong toxicity on tropical and sub-tropical agricultural and natural vegetation (Moraes et al., 2004; Felzer et al., 2007; Zhang et al., 2014; Z. Chen

et al., 2018). Ozone concentration was not measured in this study but biomass burning (Kita et al., 2000), as well as nitrogen management and isoprene emissions in oil palm plantations (Hewitt et al., 2009 and 2011), are considered to significantly affect near-surface ozone concentration due to emission of ozone precursor gases. Fire air pollution generally leads to a decrease in gross primary productivity (GPP) (Yue and Unger, 2018). To our knowledge, no study has focused on ozone concentration from biomass burning during the 2015 ENSO event, but studies observe a strong increase in ozone concentration from biomass burning during the 1997 ENSO (Thompson et al., 2001) and during the 2006 ENSO event (Nassar et al., 2009). At our study site, we therefore expect an increase in ground-level ozone concentration during the haze drought period which might have negatively affected oil palm carbon sequestration.

Increased aerosol concentration from biomass burning and the related increase in diffuse light increase plant photosynthesis and therefore decrease the ratio of sensible to latent heat (Steiner et al., 2013). However, in our study and during the peak of the drought, when forest fires started to develop in the area, we observed an increase in the ratio of sensible to latent heat (Bowen ratio) which is likely due to water stress and related partial stomata closure at high VPD (Dufrene and Saugier, 1993; Oetli et al., 2018).

Further, increased aerosol concentration is able to increase overall canopy photosynthesis under moderately enhanced diffuse light conditions (Knobl and Baldocchi, 2008; Mercado et al., 2009; Kanniah et al., 2012), and sun-exposed leaves seem to benefit from lower VPD while shaded leaves benefit from increased diffuse light conditions (Wang et al., 2018). Although our measurements and MLRM suggest that the leaves benefitted from the increase in diffuse light conditions during the haze drought period, the high level of VPD, especially during midday, was an overall stress factor for the oil palm plantation and therefore resulted in a decrease in CO<sub>2</sub> uptake. At our study site, increased fraction of diffuse radiation due to biomass burning had an overall positive impact (increase in CO<sub>2</sub> uptake) while decreased incoming PAR a negative impact on CO<sub>2</sub> uptake, which is in line with the findings of Malavelle et al. (2019). However, while the authors of that study conclude that the positive impact of increased diffuse light conditions offsets the negative impact of decreased PAR, we observe that the increase in diffuse light conditions is not able to offset the negative impact in decreased PAR. We suggest that the strong intensity and relatively long duration of the haze, with persistently high values of fraction of diffuse radiation for approx. 2 months, exceeded an optimal range of diffuse fraction (Knobl and Baldocchi, 2008) and therefore inhibited a positive impact on CO<sub>2</sub> uptake.

#### 4.2 Short-term response of oil palm to changed climatic conditions and adaptation strategies

Paterson et al. (2015) report that increasing frequency of drought in Southeast Asia has already caused a decline of 10%–30% in palm oil production. Our study supports the findings of Dufrene and Saugier (1993) and Apichatmeta et al. (2017) that short-term drought conditions and elevated irradiance under the current or potentially amplified ENSO conditions may be beneficial for oil palm growth, since we observe an increase in CO<sub>2</sub> uptake during the non-haze drought despite relatively high VPD and low soil moisture content. Our scenario of increased non-haze drought (NHD+) suggests that drought conditions may enhance CO<sub>2</sub> uptake to a certain extent, mainly due to increased incoming PAR and increased air temperature. However, our scenario does not consider a temporal prolongation of the drought or a constant increase in temperature associated with elevated temperatures as a result of global rising CO<sub>2</sub> levels. We only considered changes in the magnitude of the atmospheric and environmental parameters under the current climate conditions, which we expect to be rather constant for the current life cycle of the oil palm plantation. Therefore, we cannot rule out that this modelled positive effect of NHD+ on CO<sub>2</sub> uptake can be maintained if drought conditions remain over a longer period, but the relatively weak impact of ET / ET<sub>pot</sub> on NEE suggests that oil palm is relatively resistant to drought.

The reduced irradiance due to fire-induced haze is another stressor for oil palm since it occurs during those periods when the oil palm plantation is already negatively affected by drought and heat. Similar to NHD+, we did not include temporal changes in the length of the increased haze drought scenario (HD+) but we see that HD+ may amplify the negative impacts on oil palm NEE. Changes in ozone and aerosol concentrations caused by biomass burning have not been measured in our study but it is very likely that both had an additional negative impact on NEE (decrease in CO<sub>2</sub> uptake), which we are quantitatively not able to capture with our MLRM. Nevertheless, negative impacts of ENSO-related droughts on oil palm productivity, carbon sequestration, growth and yield are strongly coupled with the temporal and spatial occurrence of fire-induced haze and its ancillary effects, such as reduced incoming PAR, as well as air pollution of increased ozone and aerosol concentration.

It has been shown that fertilised mature commercial oil palm plantations transpire more water than tropical rainforests due to high productivity (Manoli et al., 2018), thus making them more prone to the effects of droughts (Bakoumé et al., 2013). Adaptation strategies, such as short-term irrigation or the establishment of irrigation ditches may dampen the drought-related impacts in oil palm plantations but aggravate the depletion of natural water reservoirs (Manoli et al., 2018). Elongated periods of drought, as shown in this study, increase sensible heating at the cost of evapotranspi-

ration, resulting in surface warming. Oil palm plantations have a strong potential to further amplify air heating during droughts since they are hotter and dryer compared to tropical rainforest and rubber monocultures even during non-El Niño years (Hardwick et al., 2015; Meijide et al., 2018). Covering vast areas of tropical lowlands of Sumatra and Borneo, oil palm plantations have already caused an increase in land surface temperature (Sabajo et al., 2017).

State-of-the-art process-based land surface schemes, such as the Community Land Model (CLM4.5) (Oleson et al., 2013; Fan et al., 2015), are powerful tools for addressing ecosystem surface energy balance, hydrological processes and carbon–nitrogen biogeochemistry (Oleson et al., 2013; Fan et al., 2015). Although these models are well-developed and widely used, they fail to include smoke haze as an environmental parameter affecting ecosystem behaviour. In this study, we used a simple multi-linear regression model (MLRM) to assess the impact of haze drought on oil palm productivity and developed an increased haze scenario (HD+). With this simple model we were able to show strong site-specific negative response of oil palm to haze drought. These specific results of oil palm behaviour during drought and haze conditions might be useful to parameterise models such as CLM and may even be applicable to other ecosystem and land-use types.

## 5 Conclusions

In this study, we investigate the impact of drought and smoke haze on the net CO<sub>2</sub> exchange, evapotranspiration, yield and surface energy budget in a commercial oil palm plantation. We found that drought and smoke haze conditions, with related increase in atmospheric VPD and air temperature, and changes in light conditions are major disturbing factors for oil palm plantations. Our measurements and MLRM showed that the strong haze amplified the negative effects of the drought. It is very likely that without the haze, the negative impact on CO<sub>2</sub> fluxes, carbon accumulation and yield would have been less pronounced. Although micrometeorological measurements in oil palm plantations become more and more frequent, there is still a substantial lack of air quality measurements, e.g. ozone or aerosol concentration. In our study, smoke haze may have substantially increased ozone and aerosol concentration, which both further negatively impact the oil palm plantation. Fire-preventing measures such as sustainable land management, stricter law enforcement and sanctioning, strategic hazard planning and awareness-raising of the effects of fires not only on oil palm yield but also on air quality and health may help to mitigate the negative effects of drought. Further, incorporating smoke haze as an environmental stress factor into regional or global model approaches may foster more accurate estimations of ecosystem CO<sub>2</sub>, energy and water vapour flux behaviour during such extreme meteorological events and may

allow a more holistic viewpoint of possible adaptation strategies and hazard-prevention caused by ENSO.

*Code and data availability.* The code and data used in this study are available on GitHub ([https://github.com/CbioST/ENSO\\_OilPalm](https://github.com/CbioST/ENSO_OilPalm), last access: 27 July 2019) (Stiegler and Ali, 2019).

*Supplement.* The supplement related to this article is available online at: <https://doi.org/10.5194/bg-16-2873-2019-supplement>.

*Author contributions.* The original idea of the paper was suggested by AK, AM and CS and discussed and developed by all authors. AM performed the field work and CS performed the data analysis. AAA and CS developed the model code, run the simulations and performed the model analysis. CS prepared the manuscript with contributions from all co-authors.

*Competing interests.* The authors declare that they have no conflict of interest.

*Acknowledgements.* This study was funded by the Deutsche Forschungsgemeinschaft (DFG, German Research Foundation) – project number 192626868 – SFB 990 and the Ministry of Research, Technology and Higher Education (Ristekdikti) in the framework of the collaborative German–Indonesian research project CRC990, subproject A03 and A07. The authors wish to thank our local field assistants in Indonesia, i.e. Basri, Bayu and Darwis, as well as Edgar Tunsch, Malte Puhon, Frank Tiedemann and Dietmar Fellert for their technical support. We also thank PTPN6 for giving us permission to conduct our research at the oil palm plantation.

*Financial support.* This research has been supported by the Deutsche Forschungsgemeinschaft (grant no. 192626868 – SFB 990).

This open-access publication was funded by the University of Göttingen.

*Review statement.* This paper was edited by Paul Stoy and reviewed by two anonymous referees.

## References

- Allen, K., Corre, M. D., Tjoa, A., and Veldkamp, E.: Soil Nitrogen-cycling responses to conversion of lowland forests to oil palm and rubber plantations in Sumatra, Indonesia, *PLoS ONE*, 10, e0133325, <https://doi.org/10.1371/journal.pone.0133325>, 2105.
- Apichatmeta, K., Sudsiri, C. J., and Ritchie, R. J.: Photosynthesis of oil palm (*Elaeis guineensis*), *Sci. Hortic.-Amsterdam*, 214, 34–40, <https://doi.org/10.1016/j.scienta.2016.11.013>, 2017.

- Bakoumé, C., Shahbudin, N., Yacob, S., Siang, C. S., and Thambi, M. N.: Improved method for estimating soil moisture deficit in oil palm (*Elaeis guineensis* Jacq.) areas with limited climatic data, *J. Agr. Sci.*, 5, 57–65, <https://doi.org/10.5539/jas.v5n8p57>, 2013.
- Barcelos, E., de Almeida Rios, S., Cunha, R. N., Lopes, R., Motoike, S. Y., Babiychuk, E., and Kushnir, S.: Oil palm natural diversity and the potential for yield improvement, *Front. Plant Sci.*, 6, 190, <https://doi.org/10.3389/fpls.2015.00190>, 2015.
- Bayona-Rodríguez, C. and Romero, H. M.: Estimation of transpiration in oil palm (*Elaeis guineensis* Jacq.) with the heat ratio method, *Agronomía Colombiana*, 34, 172–178, <https://doi.org/10.15446/agron.colomb.v34n2.55649>, 2016.
- Betts, R. A., Jones, C. D., Knight, J. R., Keeling, R. F., and Kennedy, J. J.: El Niño and a record CO<sub>2</sub> rise, *Nat. Clim. Change*, 6, 806–810, 2016.
- Cai, W., Borlace, S., Lengaigne, M., van Resch, P., Collins, M., Vecchi, G., and Jin, F.-F.: Increasing frequency of extreme El Niño events due to greenhouse warming, *Nat. Clim. Change*, 4, 111–116, <https://doi.org/10.1038/NCLIMATE2100>, 2014.
- Cai, W., Wang, G., Dewitte, B., Wu, L., Santoso, A., Takahashi, K., and McPhaden, M.: Increased variability of eastern Pacific El Niño under greenhouse warming, *Nature*, 564, 201–206, <https://doi.org/10.1038/s41586-018-0776-9>, 2018.
- Caliman, J. and Southworth, A.: Effect of drought and haze on the performance of oil palm, 1998 International Oil Palm Conference, Commodity of the past, today, and the future, Sheraton Nusa Indah Hotel, Bali, 23–25 September 1998, 1–40, 1998.
- Cao, H.-X., Sun, C.-X., Shao, H.-B., and Lei, X.-T.: Effects of low temperature and drought on the physiological and growth changes in oil palm seedlings, *Afr. J. Biotechnol.*, 10, 2630–2637, <https://doi.org/10.5897/AJB10.1272>, 2011.
- Chatfield, C.: Problem Solving: a Statistician's Guide, Chapman and Hall, London, UK, 1995.
- Cha-um, S., Yamda, N., Takabe, T., and Kirdmanee, C.: Physiological features and growth characters of oil palm (*Elaeis guineensis* Jacq.) in response to reduced water-deficit and rewatering, *Aust. J. Crop Sci.*, 7, 432–439, 2013.
- Chen, Z., Cao, J., Yu, H., and Shang, H.: Effects of elevated ozone levels on photosynthesis, biomass and non-structural carbohydrates of *Phoebe bournei* and *Phoebe zhennan* in subtropical China, *Front. Plant Sci.*, 9, 1764, <https://doi.org/10.3389/fpls.2018.01764>, 2018.
- Chong, K. L., Kanniah, K. D., Pohl, C., and Tan, K. P.: A review of remote sensing applications for oil palm studies, *Geo-spatial Information Science*, 20, 184–200, <https://doi.org/10.1080/10095020.2017.1337317>, 2017.
- Corley, R. H. and Tinker, P. B.: The Oil Palm, Wiley-Blackwell, Chichester, West Sussex, UK, 2016.
- Cunningham, S. C.: Photosynthetic responses to vapour pressure deficit in temperature and tropical evergreen rainforest trees of Australia, *Oecologia*, 142, 521–528, <https://doi.org/10.1007/s00442-004-1766-1>, 2005.
- Drescher, J., Rembold, K., Allen, K., Beckschäfer, P., Buchori, D., Clough, Y., and Scheu, S.: Ecological and socio-economic functions across tropical land use systems after rainforest conversion, *Philos. T. R. Soc. B*, 371, 20150275, <https://doi.org/10.1098/rstb.2015.0275>, 2016.
- Dufrene, E. and Saugier, B.: Gas exchange of oil palm in relation to light, vapour pressure deficit, temperature and leaf age, *Funct. Ecol.*, 7, 97–104, 1993.
- Falge, E., Baldocchi, D., Olson, R., Anthoni, P., Aubinet, M., Bernhofer, C., and Wofsy, S.: Gap filling strategies for defensible annual sums of net ecosystem exchange, *Agr. Forest Meteorol.*, 107, 43–69, 2001.
- Fan, Y., Rounsard, O., Bernoux, M., Le Maire, G., Panferov, O., Kotowska, M. M., and Knohl, A.: A sub-canopy structure for simulating oil palm in the Community Land Model (CLM-Palm): phenology, allocation and yield, *Geosci. Model Dev.*, 8, 3785–3800, <https://doi.org/10.5194/gmd-8-3785-2015>, 2015.
- Felzer, B. S., Cronin, T., Reilly, J. M., Melillo, J. M., and Wang, X.: Impacts of ozone on trees and crops, *C. R. Geosci.*, 339, 784–798, <https://doi.org/10.1016/j.crte.2007.08.008>, 2007.
- Hardwick, S. R., Toumi, R., Pfeifer, M., Turner, E. C., Nilus, R., and Ewers, R. M.: The relationship between leaf area index and microclimate in tropical forest and oil palm plantation: Forest disturbance drives changes in microclimate, *Agr. Forest Meteorol.*, 201, 187–195, <https://doi.org/10.1016/j.agrformet.2014.11.010>, 2015.
- Henson, I. E.: Modelling the effects of “haze” on oil palm productivity and yield, *J. Oil Palm Res.*, 12, 123–134, 2000.
- Henson, I. E. and Harun, M. H.: Carbon dioxide enrichment in oil palm canopies and its possible influence on photosynthesis, *Oil Palm Bulletin*, 51, 10–19, 2005a.
- Henson, I. E. and Harun, M. H.: The influence of climatic conditions on gas and energy exchanges above a young oil palm stand in North Kendah, Malaysia, *J. Oil Palm Res.*, 17, 73–91, 2005b.
- Heuvelink, T. L., Dueck, T. A., Janse, J., Gort, G., and Marcelis, L. F.: Enhancement of crop photosynthesis by diffuse light: quantifying the contributing factors, *Ann. Bot.-London*, 114, 145–156, <https://doi.org/doi:10.1093/aob/mcu071>, 2014.
- Hewitt, C. N., MacKenzie, A. R., Di Carlo, P., Di Marco, C. F., Dorsey, J. R., Evans, M., Fowler, D., Gallagher, M. W., Hopkings, J. R., Jones, C. E., Langford, B., Lee, J. D., Lewis, A. C., Lim, S. F., McQuaid, J., Misztal, P., Moller, S. J., Monks, P. S., Nemitz, E., Oram, D. E., Owen, S. M., Phillips, G. J., Pugh, A. M., Pyle, J. A., Reeves, C. E., Ryder, J., Siong, J., Skiba, U., and Stewart, D. J.: Nitrogen management is essential to prevent tropical oil palm plantations from causing ground-level ozone pollution, *P. Natl. Acad. Sci. USA*, 106, 18447–18451, 2009.
- Hewitt, C. N., Ashworth, K., Boynard, A., Guenther, A., Langford, B., MacKenzie, A. R., Misztal, P. K., Nemitz, E., Owen, S. M., Possell, M., Pugh, T. A. M., Ryan, A. C., and Wild, O.: Ground-level ozone influenced by circadian control of isoprene emissions, *Nat. Geosci.*, 4, 671–674, <https://doi.org/10.1038/NNGEO1271>, 2011.
- Huijnen, V., Wooster, M. J., Kaier, J. W., Gaveau, D. L., Flemming, J., Parrington, M., and van Wee, M.: Fire carbon emissions over maritime southeast Asia in 2015 largest since 1997, *Sci. Rep.-UK*, 6, 26886, <https://doi.org/10.1038/srep26886>, 2016.
- Ibrahim, M. H., Jaafar, H. Z., Harun, M. H., and Yusop, M. R.: Changes in growth and photosynthetic patterns of oil palm (*Elaeis guineensis* Jacq.) seedlings exposed to short-term CO<sub>2</sub> enrichment in a closed top chamber, *Acta Physiol.*, 32, 305–313, 2010.
- IPCC: Climate Change 2013: The physical science basis, Contribution of working group I to the fifth assessment report

- of the intergovernmental panel on climate change, edited by: Stocker, T. F., Qin, D., Plattner, G.-K., and Midgley, P. M., Cambridge University Press, Cambridge, UK, <https://doi.org/10.1017/CBO9781107415324>, 2013.
- Jaafar, H. Z. and Ibrahim, M. H.: Photosynthesis and quantum yield of oil palm juveniles to elevated carbon dioxide, in: *Advances Photosynthesis Fundamental Aspects*, edited by: Najafpour, M. M., InTechPubl, Rijeka, Croatia, 321–340, <https://doi.org/10.5772/26167>, 2012.
- Jazayeri, S. M., Rivera, Y. D., Camperos-Reyes, J. E., and Romero, H. M.: Physiological effects of water deficit on two oil palm (*Elaeis guineensis* Jacq.) genotypes, *Agronomia Colombiana*, 33, 164–173, <https://doi.org/10.15446/agron.colomb.v33n2.49846>, 2015.
- Jiménez-Muñoz, J. C., Mattar, C., Barichivich, J., Santamaria-Artigas, A., Takahashi, K., Malhi, Y., and Schrier, G.: Record-breaking warming and extreme drought in the Amazon rainforest during the course of El Niño 2015–2016, *Sci. Rep.-UK*, 6, 33130, 2016.
- Kanniah, K. D., Beringer, J., North, P., and Hutley, L.: Control of atmospheric particles on diffuse radiation and terrestrial plant productivity: A review, *Prog. Phys. Geog.*, 36, 209–237, <https://doi.org/10.1177/0309133311434244>, 2012.
- Keupp, L., Pollinger, F., and Paeth, H.: Assessment of future ENSO changes in a CMIP3/CMIP5 multi-model and multi-index framework, *Int. J. Climatol.*, 37, 3439–3451, <https://doi.org/10.1002/joc.4928>, 2017.
- Kim, S. T., Cai, W., Jin, F.-F., Santoso, A., Wu, L., and Guillard, E.: Response of El Niño sea surface temperature variability to greenhouse warming, *Nat. Clim. Change*, 786–790, <https://doi.org/10.1038/NCLIMATE2326>, 2014.
- Kita, K., Fujiwara, M., and Kawakami, S.: Total ozone increase associated with forest fires over the Indonesian region and its relation to the El Niño-southern oscillation, *Atmos. Environ.*, 34, 2681–2690, 2000.
- Knohl, A. and Baldocchi, D. D.: Effects of diffuse radiation on canopy gas exchange processes in a forest ecosystem, *J. Geophys. Res.*, 113, G02023, <https://doi.org/10.1029/2007JG000663>, 2008.
- Koh, L. P. and Ghazoul, J.: Biofuels, biodiversity, and people: Understanding the conflicts and finding opportunities, *Biol. Conserv.*, 141, 2450–2460, <https://doi.org/10.1016/j.biocon.2008.08.005>, 2008.
- Koh, L. P., Miettinen, J., Liew, S. C., and Ghazoul, J.: Remotely sensed evidence of tropical peatland conversion to oil palm, *P. Natl. Acad. Sci. USA*, 108, 5127–5132, <https://doi.org/10.1073/pnas.1018776108>, 2011.
- Kozlov, V. S., Yausheva, E. P., Terpigova, S. A., Panchenko, M. V., Chernov, D. G., and Shmargunov, V. P.: Optical-microphysical properties of smoke haze from Siberian forest fires in summer 2012, *Int. J. Remote Sens.*, 35, 5722–5741, 2014.
- Lamade, E. and Bouillet, J.-P.: Carbon storage and global change: the role of oil palm, Oilseeds and fats, *Crops and Lipids*, 12, 154–160, 2005.
- Legros, S., Mialet-Serra, I., Caliman, J.-P., Siregar, F. A., Clément-Vidal, A., and Dingkuhn, M.: Phenology and growth adjustments of oil palm (*Elaeis guineensis*) to photoperiod and climate variability, *Ann. Bot.-London*, 104, 1171–1182, <https://doi.org/10.1093/aob/mcp214>, 2009.
- Lim, Y.-K., Kovach, R. M., Pawson, S., and Vernieres, G.: The 2015/16 El Niño event in context of the MERRA-2 reanalysis: a comparison of the tropical Pacific with 1982/83 and 1997/98, *J. Climate*, 30, 4819–4842, <https://doi.org/10.1175/JCLI-D-16-0800.1>, 2017.
- Maillard, G., Ochs, R., and Daniel, C.: Analysis of the effects of drought on the oil palm, *Oleagineux*, 29, 397–404, 1974.
- Malavelle, F. F., Haywood, J. M., Mercado, L. M., Folberth, G. A., Bellouin, N., Sitch, S., and Artaxo, P.: Studying the impact of biomass burning aerosol radiative and climate effects on the Amazon rainforest productivity with an Earth system model, *Atmos. Chem. Phys.*, 19, 1301–1326, <https://doi.org/10.5194/acp-19-1301-2019>, 2019.
- Manoli, G., Mejjide, A., Huth, N., Knohl, A., Kosugi, Y., Burdando, P., and Fatichi, S.: Ecohydrological changes after tropical forest conversion to oil palm, *Environ. Res. Lett.*, 13, 064035, <https://doi.org/10.1088/1748-9326/aac54e>, 2018.
- Mathews, J. and Ardiyanto, A.: Impact of forest fire induces haze on oil extraction rate (OER) in Central Kalimantan province, *Journal of Oil Palm, Environment and Health*, 7, 28–33, <https://doi.org/10.5366/jope.2016.03>, 2016.
- Matysek, M., Evers, S., Samuel, M. K., and Sjogersten, S.: High heterotrophic CO<sub>2</sub> emissions from a Malaysian oil palm plantations during dry-season, *Wetl. Ecol. Manag.*, 26, 415–424, <https://doi.org/10.1007/s11273-017-9583-6>, 2018.
- Mejjide, A., Röhl, A., Fan, Y., Herbst, M., Niu, F., Tiedemann, F., and Knohl, A.: Controls of water and energy fluxes in oil palm plantations: Environmental variables and oil palm age, *Agr. Forest Meteorol.*, 239, 71–85, <https://doi.org/10.1016/j.agrformet.2017.02.034>, 2017.
- Mejjide, A., Badu, C. S., Moyano, F., Tiralla, N., Gunawan, D., and Knohl, A.: Impact of forest conversion to oil palm and rubber plantations on microclimate and the role of the 2015 ENSO event. *Agr. Forest Meteorol.*, 252, 208–219, <https://doi.org/10.1016/j.agrformet.2018.01.013>, 2018.
- Méndez, Y. D. R., Chacón, L. M., Bayona, C. J., and Romero, H. M.: Physiological response of oil palm interspecific hybrids (*Elaeis oleifera* H. N. K. Cortes versus *Elaeis guineensis* Jacq.) to water deficit, *Brazilian Society of Plant Physiology*, 24, 273–280, <https://doi.org/10.1590/S1677-04202012000400006>, 2012.
- Mercado, L. M., Bellouin, N., Sitch, S., Boucher, O., Huntingford, C., Wild, M., and Cox, P. M.: Impact of changes in diffuse radiation on the global land carbon sink, *Nature*, 458, 1014–1017, <https://doi.org/10.1038/nature07949>, 2009.
- Moraes, R. M., Furlan, C. M., Bulbovas, P., Domingos, M., Meirelles, S. T., Salatino, A., Delitti, W. B. C., and Sanz, M. J.: Photosynthetic responses of tropical trees to short-term exposure to ozone, *Photosynthetica*, 42, 291–293, 2004.
- Moreira, D. S., Longo, K. M., Freitas, S. R., Yamasoe, M. A., Mercado, L. M., Rosário, N. E., Gloor, E., Viana, R. S. M., Miller, J. B., Gatti, L. V., Wiedemann, K. T., Domingues, L. K. G., and Correia, C. C. S.: Modeling the radiative effects of biomass burning aerosols on carbon fluxes in the Amazon region, *Atmos. Chem. Phys.*, 17, 14785–14810, <https://doi.org/10.5194/acp-17-14785-2017>, 2017.
- Nassar, R., Logan, J. A., Megretskaia, I. A., Murray, L. T., Zang, L., and Jones, D. B. A.: Analysis of tropical tropospheric ozone, carbon monoxide, and water vapour during the 2006 El Niño using

- TES observations and the GEOS-Chem model, *J. Geophys. Res.*, 114, D17304, <https://doi.org/10.1029/2009JD011760>, 2009.
- Neelin, J. D., Münnich, M., Su, H., Meyerson, J. E., and Holloway, C. E.: Tropical drying trends in global warming models and observations. *P. Natl. Acad. Sci.*, 103, 6110–6115, 2006.
- Niu, F., Röhl, A., Hardanto, A., Meijide, A., Köhler, M., Hendrayanto, and Hölscher, D.: Oil palm water use: calibration of a sap flux method and a field measurement scheme, *Tree Physiol.*, 35, 563–573, <https://doi.org/10.1093/treephys/tpv013>, 2015.
- Noor, M. R., Harun, M. H., and Jantan, N. M.: Physiological plant stress and responses in oil palm, *Oil Palm Bulletin*, 62, 25–32, 2011.
- Oettli, P., Behera, S. K., and Yamagata, T.: Climate based predictability of oil palm tree yield in Malaysia, *Sci. Rep.-UK*, 8, 2271, <https://doi.org/10.1038/s41598-018-20298-0>, 2018.
- Olchev, A., Ibrom, A., Panferov, O., Gushchina, D., Kreilein, H., Popov, V., Propastin, P., June, T., Rauf, A., Gravenhorst, G., and Knohl, A.: Response of CO<sub>2</sub> and H<sub>2</sub>O fluxes in a mountainous tropical rainforest in equatorial Indonesia to El Niño events, *Biogeosciences*, 12, 6655–6667, <https://doi.org/10.5194/bg-12-6655-2015>, 2015.
- Oleson, K. W., Lawrence, D. M., Bonan, G. B., Drewniak, B., Huang, M., Koven, C. D., and Yang, Z.-L.: Technical description of version 4.5 of the Community Land Model (CLM), National Center for Atmospheric Research, Boulder, CO, USA, <https://doi.org/10.5065/D6RR1W7M>, 2013.
- Paterson, R., Sariah, M., and Lima, N.: How will climate change affect oil palm fungal diseases?, *Crop Prot.*, 46, 113–120, <https://doi.org/10.1016/j.cropro.2012.12.023>, 2013.
- Paterson, R., Kumar, L., Taylor, S., and Lima, N.: Future climate effects on suitability for growth of oil palms in Malaysia and Indonesia, *Sci. Rep.-UK*, 5, 14457, <https://doi.org/10.1038/srep14457>, 2015.
- Paterson, R., Kumar, L., Shabani, F., and Lima, N.: World climate suitability projections to 2050 and 2100 for growing oil palm, *J. Agr. Sci.*, 155, 689–702, <https://doi.org/10.1017/S0021859616000605>, 2017.
- Pirker, J., Mosnier, A., Kraxner, F., Havlík, P., and Obersteiner, M.: What are the limits to oil palm expansion?, *Global Environ. Chang.*, 40, 73–81, <https://doi.org/10.1016/j.gloenvcha.2016.06.007>, 2016.
- Power, S., Delage, F., Chung, C., Kociuba, G., and Keay, K.: Robust twenty-first-century projections of El Niño and related precipitation variability, *Nature*, 502, 541–547, <https://doi.org/10.1038/nature12580>, 2013.
- Rasmusson, E. M. and Carpenter, T. H.: Variations in tropical sea surface temperature and surface wind fields associated with the Southern Oscillation/El Niño, *Mon. Weather Rev.*, 110, 354–384, 1981.
- Ray-Mukherjee, J., Nimon, K., Mukherjee, S., Morris, D. W., Slotow, R., and Hamer, M.: Using commonality analysis in multiple regressions: a tool to decompose regression effects in the face of multicollinearity, *Methods Ecol. Evol.*, 5, 320–328, <https://doi.org/10.1111/2041-210x.12166>, 2014.
- Reichstein, M., Falge, E., Baldocchi, D., Papale, D., Aubinet, M., Berbigier, P., Brnohofer, C., Buchmann, N., Gilmanov, T., Granier, A., Grünwald, T., Havránková, K., Ilvesniemi, H., Janous, D., Knohl, A., Laurila, T., Lohila, A., Loustau, D., Matteucci, G., Meyers, T., Miglietta, F., Ourcival, J.-M., Pumpanen, J., Rambal, S., Rotenberg, E., Sanz, M., Tenhunen, J., Seufert, G., Vaccari, F., Vesala, T., Yakir, D., and Valentini, R.: On the separation of net ecosystem exchange into assimilation and ecosystem respiration: review and improved algorithm, *Glob. Change Biol.*, 11, 1424–1439, <https://doi.org/10.1111/j.1365-2486.2005.001002.x>, 2005.
- Rowland, L., da Costa, A. C., Galraith, D. R., Oliveira, R. S., Binks, O. J., Oliveira, A. A., and Meir, P.: Death from drought in tropical forests is triggered by hydraulics not carbon starvation, *Nature*, 528, 119–124, <https://doi.org/10.1038/nature15539>, 2015.
- Sabajo, C. R., le Maire, G., June, T., Meijide, A., Rouspard, O., and Knohl, A.: Expansion of oil palm and other cash crops causes an increase of the land surface temperature in the Jambi province in Indonesia, *Biogeosciences*, 14, 4619–4635, <https://doi.org/10.5194/bg-14-4619-2017>, 2017.
- Santoso, A., McPhaden, M. J., and Cai, W.: The defining characteristics of ENSO extremes and the strong 2015/2016 El Niño, *Rev. Geophys.*, 55, 1079–1129, <https://doi.org/10.1002/2017RG000560>, 2017.
- Sellers, P. J., Mintz, Y., Sud, Y. C., and Dalcher, A.: A simple biosphere model (SiB) for use within General Circulation Models, *J. Atmos. Sci.*, 43, 505–531, 1986.
- Sigau, C. U. and Hamid, H. A.: Soil CO<sub>2</sub> efflux of oil palm and rubber plantation in 6-year-old and 22-year-old chronosequence, *Pertanika Journal of Tropical Agricultural Science*, 41, 1217–1231, 2018.
- Slot, M., Rey-Sánchez, C., Gerber, S., Lichstein, J. W., Winter, K., and Kitajima, K.: Thermal acclimation of leaf respiration of tropical trees and lianas: response to experimental canopy warming, and consequences for tropical carbon balance, *Glob. Change Biol.*, 20, 2915–2926, <https://doi.org/10.1111/gcb.12563>, 2014.
- Steiner, A. L., Mermelstein, D., Cheng, S. J., Twine, T. E., and Oliphant, A.: Observed impact of atmospheric aerosols on the surface energy budget, *Earth Interact.*, 17, 1–22, <https://doi.org/10.1175/2013EI000523.1>, 2013.
- Stiegler, C. and Ali, A. A.: Model code and meteorological data, available at: [https://github.com/CbioST/ENSO\\_OilPalm](https://github.com/CbioST/ENSO_OilPalm), last access: 27 July 2019.
- Sun, C., Ca, H., Shao, H., Lei, X., and Xiao, Y.: Growth and physiological responses to water and nutrient stress in oil palm, *Afr. J. Biotechnol.*, 10, 10465–10471, <https://doi.org/10.5897/AJB11.463>, 2011.
- Tangang, F.: Climate change: is Southeast Asia up to the challenge?: the roles of climate variability and climate change on smoke haze occurrences in Southeast Asia region, edited by: Kitchen, N., London School of Economics and Political Science, London, UK, 2010.
- Thompson, A. M., Witte, J. C., Hudson, R. D., Guo, H., Herman, J. R., and Fujiwara, M.: Tropical tropospheric ozone and biomass burning, *Science*, 291, 2128–2132, 2001.
- Turner, P. A., Field, C. B., Lobell, D. B., Sanchez, D. L., and Mach, K. J.: Unprecedented rates of land-use transformation in modelled climate change mitigation pathways, *Nature Sustainability*, 1, 240–245, <https://doi.org/10.1038/s41893-018-0063-7>, 2018.
- Urban, O., Klem, K., Holišová, P., Šigut, L., Šprtová, M., Teslová-Navrátlová, P., and Grace, J.: Impact of elevated CO<sub>2</sub> concentration on dynamics of leaf photosynthesis in *Fagus sylvatica* is modulated by sky conditions, *Environ. Pollut.*, 185, 271–280, <https://doi.org/10.1016/j.envpol.2013.11.009>, 2014.

- USDA: Oilseeds: World markets and trade, Foreign Agricultural Service, United States Department of Agriculture, Washington: United States Department of Agriculture, available at: <https://apps.fas.usda.gov/psdonline/circulars/oilseeds.pdf> (last access: 26 July 2019), 2018.
- Wahid, M. B., Abdullah, S. N., and Henson, I.: Oil palm achievements and potential, *Plant Prod. Sci.*, 8, 288–297, <https://doi.org/10.1626/pps.8.288>, 2005.
- Wang, X., Wu, J., Chen, M., Xu, X., Wang, Z., Wang, B., Wang, C., Piao, S., Lin, W., Miao, G., Deng, M., Qiao, C., Wang, J., Xu, S., and Liu, L.: Field evidences for the positive effects of aerosols on tree growth, *Glob. Change Biol.*, 24, 4983–4992, <https://doi.org/10.1111/gcb.14339>, 2018.
- Whittingham, M. J., Stephens, P. A., Bradbury, R. B., and Freckleton, R. P.: Why do we still use stepwise modelling in ecology and behaviour?, *J. Anim. Ecol.*, 75, 1182–1189, <https://doi.org/10.1111/j.1365-2656.2006.01141.x>, 2006.
- Woittiez, L. S., van Wijk, M. T., Slingerland, M., van Noordwijk, M., and Giller, K. E.: Yields in oil palm: A quantitative review of contributing factors, *Eur. J. Agron.*, 83, 57–77, <https://doi.org/10.1016/j.eja.2016.11.002>, 2017.
- Wolter, K.: The Southern Oscillation in surface circulation and climate over the tropical Atlantic, eastern Pacific, and Indian Oceans as captured by cluster analysis, *J. Clim. Appl. Meteorol.*, 26, 540–558, 1986.
- Wolter, K. and Timlin, M. S.: El Niño/Southern Oscillation behaviour since 1871 as diagnosed in an extended multivariate ENSO index (MEI.ext), *Int. J. Climatol.*, 31, 1074–1087, <https://doi.org/10.1002/joc.2336>, 2011.
- Yamasoe, M. A., von Randow, C., Manzi, A. O., Schafer, J. S., Eck, T. F., and Holben, B. N.: Effect of smoke and clouds on the transmissivity of photosynthetically active radiation inside the canopy, *Atmos. Chem. Phys.*, 6, 1645–1656, <https://doi.org/10.5194/acp-6-1645-2006>, 2006.
- Yue, X. and Unger, N.: Fire air pollution reduces global terrestrial productivity, *Nat. Commun.*, 9, 5413, <https://doi.org/10.1038/s41467-018-07921-4>, 2018.
- Zhang, W., Feng, Z., Wang, X., and Niu, J.: Elevated ozone negatively affects photosynthesis of current-year leaves but not previous-year leaves in evergreen *Cyclobalanopsis glauca* seedlings, *Environ. Pollut.*, 184, 676–681, <https://doi.org/10.1016/j.envpol.2013.04.036>, 2014.
- Zhou, Z., Jiang, L., Du, E., Hu, H., Li, Y., Chen, D., and Fang, J.: Temperature and substrate availability regulate soil respiration in the tropical mountain rainforests, Hainan Island, China, *J. Plant Ecol.*, 6, 325–334, <https://doi.org/10.1093/jpe/rtt034>, 2013.
- Zuur, A. F., Ieno, E. N., and Elphick, C. S.: A protocol for data exploration to avoid common statistical problems, *Methods Ecol. Evol.*, 1, 3–14, <https://doi.org/10.1111/j.2041-210X.2009.00001.x>, 2010.